

Qin Xu<sup>1\*</sup>, Li Wei<sup>2</sup> and Kang Nai<sup>2</sup><sup>1</sup>NOAA/National Severe Storms Laboratory, Norman, Oklahoma<sup>2</sup>Cooperative Institute for Mesoscale Meteorological Studies, University of Oklahoma

## 1. Introduction

A computationally efficient two-dimensional variational method was developed by Xu et al. (2015) to analyze vortex wind fields of tornadoic mesocyclones observed by operational WSR-88D radars for nowcast applications. In this method, the vortex wind field is retrieved in a nested domain over the mesocyclone area in a moving coordinate system co-centered the mesocyclone on the lowest sweep of radar scan. As the background error covariance is formulated with the desired vortex flow dependence, the method can retrieve the vortex winds of mesocyclones scanned from a single Doppler radar. To take the advantages provided by the rapid scans of phased array radar (PAR), the method is extended by including the advection equations of radar image pattern movements as additional constraints in the cost-function, so it can use PAR rapid scans on multiple consecutive time levels (instead of single time level) to extract additional information on vortex winds from image pattern movements. The method is described in the next section.

## 2. Extended Method

### a. Vortex-flow-dependent background error covariance

As shown in sections 3b-3c of X15, the background error covariance suitable for analyzing vortex winds in radar observed tornadoic mesocyclones can be derived with desired vortex flow dependences, and the derived covariance matrix has the decomposed form of

$$\mathbf{B} = (\sigma_R \mathbf{P}, \sigma_T \mathbf{P})^{\text{diag}} (\sigma_R \mathbf{P}^T, \sigma_T \mathbf{P}^T)^{\text{diag}}, \quad (1)$$

where  $\mathbf{B}^{1/2} \equiv (\sigma_R \mathbf{P}, \sigma_T \mathbf{P})^{\text{diag}}$  is a root square of  $\mathbf{B}$  satisfying  $\mathbf{B}^{1/2} \mathbf{B}^{1/2T} = \mathbf{B}$ ,  $( )^T$  denotes the transpose of  $( )$ ,  $\sigma_R^2$  (or  $\sigma_T^2$ ) is the background error variance for the vortex-relative radial-component (or tangential-component) velocity in the moving coordinate system co-centered the mesocyclone, and  $\mathbf{P}$  is the square root of correlation matrix formulated by a vortex-flow-dependent correlation function [see (21) of X15]. Using the vortex-flow-dependent background error covariance matrix formulated in (1), the cost-function can be pre-conditioned into the following compact form [see (22) of X15]:

$$J = |\mathbf{c}'|^2/2 + |\mathbf{H}' \mathbf{c}' - \mathbf{d}/\sigma_o|^2/2, \quad (2)$$

where  $\mathbf{H}' = \sigma_o^{-1} \mathbf{H} \mathbf{B}^{1/2}$  is the  $\sigma_o$ -scaled radial-velocity observation operator for the transformed control vector  $\mathbf{c}' \equiv (\mathbf{c}_R^T, \mathbf{c}_T^T)^T$ , and  $\mathbf{c}_R$  (or  $\mathbf{c}_T$ ) is related to the state vector of the vortex-relative radial (or tangential) velocity incremental field by  $\mathbf{a}_R = \sigma_R \mathbf{P} \mathbf{c}_R$  (or  $\mathbf{a}_T = \sigma_T \mathbf{P} \mathbf{c}_T$ ). The method of X15 can be extended by incorporating  $\mathbf{B}$  formulated in (1) into the simple adjoint (SA) method (Qiu and Xu 1992) as shown in section 2c.

### b. SA method

The SA method uses the reflectivity as a tracer, with its advection equation formulated as a weak constraint in the cost-function, to retrieve the wind field from radar scanned reflectivity pattern movements. The method was upgraded by using a recursive filter (Purser et al. 2003) to efficiently compute the background error covariance, and the upgraded SA method was applied to PAR rapid scans of storm-generated microbursts (Qiu et al. 2013). In the upgraded SA method, the cost-function has the following form:

$$J = |\mathbf{c}|^2 + \tau^{-1} \int dt |\mathbf{H} \mathbf{c} - \mathbf{d}|^2 / \sigma_{ov}^2 + \tau^{-1} \int dt |\mathbf{F}(\mathbf{c}) - \mathbf{y}|^2 / (\sigma_F^2 + \sigma_o^2), \quad (3)$$

where  $\mathbf{c} \equiv (\mathbf{u}_c^T, \mathbf{v}_c^T, \mathbf{s}_c^T)^T$  is the control vector,  $\mathbf{c} = (\mathbf{u}_c^T, \mathbf{v}_c^T)^T$ ,  $\mathbf{H}$  (or  $\mathbf{d}$ ) is the observation operator (or innovation vector) for radar-observed radial velocity,  $\tau^{-1} \int dt ( )$  denotes the time average of  $( )$  over  $\tau$  – the analysis time window,  $\sigma_{ov}^2$  is the radial-velocity observation error variance,  $\mathbf{F}( )$  denotes the nonlinear observation operator that uses  $\mathbf{c}$  to integrate the reflectivity advection equation,  $\mathbf{y}$  is the observation vector for radar-observed reflectivity over the analysis time window,  $\sigma_F^2$  is the error variance for  $\mathbf{F}( )$ , and  $\sigma_o^2$  is the reflectivity observation error variance.

The control vector in (3) is subject to the following transformations:

$$\mathbf{u}_a = \sigma_b \mathbf{G} \mathbf{u}_c, \quad \mathbf{v}_a = \sigma_b \mathbf{G} \mathbf{v}_c, \quad \mathbf{s}_a = \sigma_s \mathbf{G}_s \mathbf{s}_c, \quad (4)$$

where  $\mathbf{u}_a$  (or  $\mathbf{v}_a$ ) is the state vectors of analyzed time-mean velocity incremental field  $\Delta u$  (or  $\Delta v$ ),  $\mathbf{s}_a$  is the state vector of analyzed time-mean source field  $S$  in the reflectivity advection equation,  $\sigma_b^2$  (or  $\sigma_s^2$ ) is the background error variance for  $\Delta u$  and  $\Delta v$  (or  $S$ ), and  $\mathbf{G}$  (or  $\mathbf{G}_s$ ) is the square root of background error correlation matrix for  $\Delta u$  or  $\Delta v$  (or  $S$ ) modeled by an isotropic Gaussian function and computed by the recursive filter.

### c. Extended method

The vortex-flow-dependent background error covariance  $\mathbf{B}$  formulated in (1) can be incorporated into the cost-function in (3) by expanding the control vectors  $\mathbf{c}$  and  $\mathbf{c}_\cdot$  defined in (3) to  $\mathbf{c} \equiv (\mathbf{c}_R^T, \mathbf{c}_T^T, \mathbf{c}_s^T, \mathbf{u}_c^T, \mathbf{v}_c^T, \mathbf{s}_c^T)^T$  and  $\mathbf{c}_\cdot = (\mathbf{c}_R^T, \mathbf{c}_T^T, \mathbf{u}_c^T, \mathbf{v}_c^T)^T$ , respectively. Here, the three new component vectors,  $\mathbf{c}_R$ ,  $\mathbf{c}_T$  and  $\mathbf{c}_s$ , are subject to the following transformations:

$$\mathbf{a}_R = \sigma_R \mathbf{P} \mathbf{c}_R, \quad \mathbf{a}_T = \sigma_T \mathbf{P} \mathbf{c}_T, \quad \mathbf{s}_+ = \sigma_s \mathbf{P} \mathbf{c}_s, \quad (5)$$

$$(\mathbf{u}_+^T, \mathbf{v}_+^T)^T = [(\mathbf{\Lambda}_c, -\mathbf{\Lambda}_s)^T, (\mathbf{\Lambda}_s, \mathbf{\Lambda}_c)^T] (\mathbf{a}_R^T, \mathbf{a}_T^T)^T, \quad (6)$$

where  $\mathbf{P}$  is the same square root of correlation matrix as that formulated in (1),  $\mathbf{a}_R$  (or  $\mathbf{a}_T$ ) is the same state vector as that introduced in (2) but represents the time-mean (averaged over  $\tau$ ) vortex-relative radial (or tangential) velocity incremental field, and  $\mathbf{\Lambda}_c$  (or  $\mathbf{\Lambda}_s$ ) is a diagonal matrix with its  $i^{\text{th}}$  diagonal element given by  $x_i/r_i$  (or  $y_i/r_i$ ) for  $r_i = |(x_i, y_i)|$  corresponding to the  $i^{\text{th}}$  grid point in the analysis domain co-centered with

\*Corresponding author address: Qin Xu, National Severe Storms Laboratory, 120 David L. Boren Blvd., Norman, OK 73072-7326; E-mail: Qin.Xu@noaa.gov

the vortex [see (11) of X15]. The state vectors computed from the new control vector components are combined with those computed in (4) as follows:

$$\begin{aligned}\mathbf{u} &= \mathbf{\Lambda}\mathbf{u}_+ + (\mathbf{I} - \mathbf{\Lambda})\mathbf{u}_{\text{ds}}, \\ \mathbf{v} &= \mathbf{\Lambda}\mathbf{v}_+ + (\mathbf{I} - \mathbf{\Lambda})\mathbf{v}_{\text{ds}}, \\ \mathbf{s} &= \mathbf{\Lambda}\mathbf{s}_+ + (\mathbf{I} - \mathbf{\Lambda})\mathbf{s}_{\text{ds}},\end{aligned}$$

where  $\mathbf{\Lambda}$  is a diagonal matrix with its diagonal elements given between 0 and 1 as a smooth function of  $(x, y)$ , and  $\mathbf{I}$  is the identity matrix. For simplicity, we set  $\mathbf{\Lambda} = \lambda\mathbf{I}$  with  $1 \geq \lambda \geq 0$ . For  $\lambda = 1$ , the vortex-flow-dependent background error covariance matrix formulated in (1) is fully incorporated into the cost-function in place of the original background error covariance matrix (modeled by an isotropic Gaussian function and computed by the recursive filter) in the SA method. For  $\lambda = 0$ , the method reduces to the SA method.

### 3. Applying to PAR scanned tornadic mesocyclone

The extended method is applied to NSSL PAR scans (from 19:52 to 20:35 UTC) of the tornadic mesocyclone that struck Moore in Oklahoma on 20 May 2013. Examples of retrieved vortex wind fields are shown in Fig. 1a for the extended method ( $\lambda = 1$ ) and Fig. 1b for the SA method ( $\lambda = 0$ ). The vortex wind field retrieved by the extended method in Fig. 1a is more accurate than that by the SA method in Fig. 1b, since the former compares better (than the latter) with the dual-Doppler retrieved vortex wind field in Fig. 2 of Xu et al. (2017a), especially in the vortex core area and around the curved convergence zone to the southeast side of the vortex. To test the method quantitatively, model-simulated vortex wind and reflectivity fields are used in the next section, where simulated PAR radial-velocity observations are also used as a trace field [with its advection equation added to the cost-function as a weak constraint similar to the last term in (3) for the reflectivity tracer].

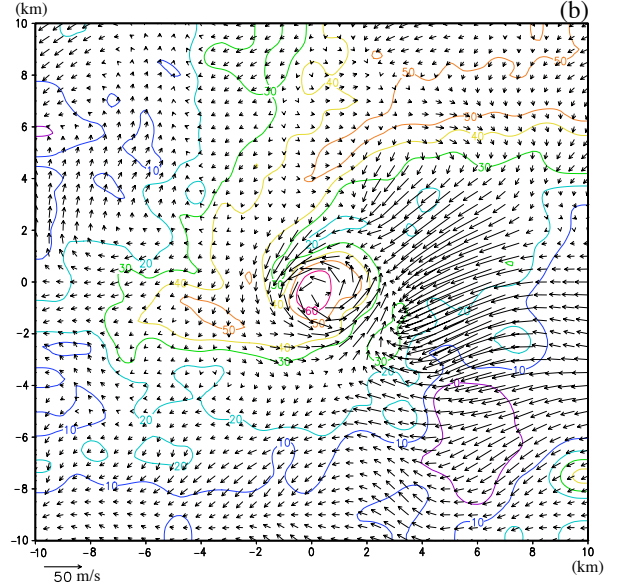
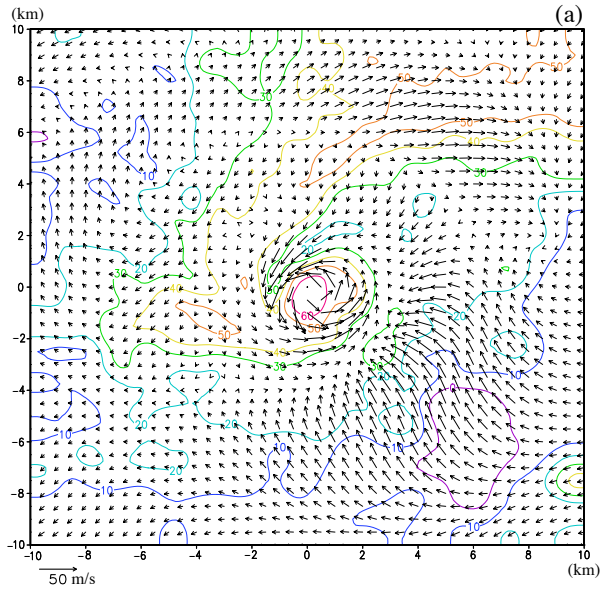


Fig. 1. Time-mean vortex winds (plotted by black arrows) retrieved in a moving coordinate system co-centered with the vortex on the conical surface of  $0.5^\circ$  sweep by (a) the extended method ( $\lambda = 1$ ) and (b) SA method ( $\lambda = 0$ ) from three consecutive PAR scans of Oklahoma Moore tornadic mesocyclone at 20:04:40, 20:06:17 and 20:07:27 UTC on 20 May 2013. The color contours plot the reflectivity (in dBZ).

### 4. Tests with simulated tornadic mesocyclone

Model-simulated vortex wind and reflectivity fields at grid spacing of  $\Delta x = 0.5$  km saved every 10 s around 19:52 UTC (from a selected single-member run in the ensemble forecasts of 20 May 2013 Oklahoma tornadic storms, produced by Snook et al. 2016) are used to generate simulated PAR radial-velocity and reflectivity observations over each selected time period  $\tau$ . Fig. 2a plots simulated true vortex winds (black arrows) averaged over  $\tau = 60$  s in the moving coordinate system co-centered with the vortex at 0.2 km height. Fig. 2b plots the retrieved time-mean vortex winds (black arrows) versus those (duplicated by green arrows) in Fig. 1a. The RMS error of the retrieved vortex winds in Fig. 2b is listed (4.59 m/s) in Table 1 versus the RMS errors obtained by using 0, 1 or 2 traces with  $\lambda = 0, 0.5$  or 1. As listed in Table 1, the RMS error can be reduced by using tracers (reflectivity and/or radial-velocity) and  $\mathbf{B}$  in (1) ( $\lambda = 1$  or 0.5).

Table 1. RMS errors (in  $\text{ms}^{-1}$ ) of vortex winds retrieved by using 0, 1 or 2 traces with  $\lambda = 0, 0.5$  or 1.

	No tracer	1 tracer	2 tracer
$\lambda = 0$	7.55	5.58	5.10
$\lambda = 0.5$	6.20	5.31	4.59
$\lambda = 1$	5.87	5.65	5.02

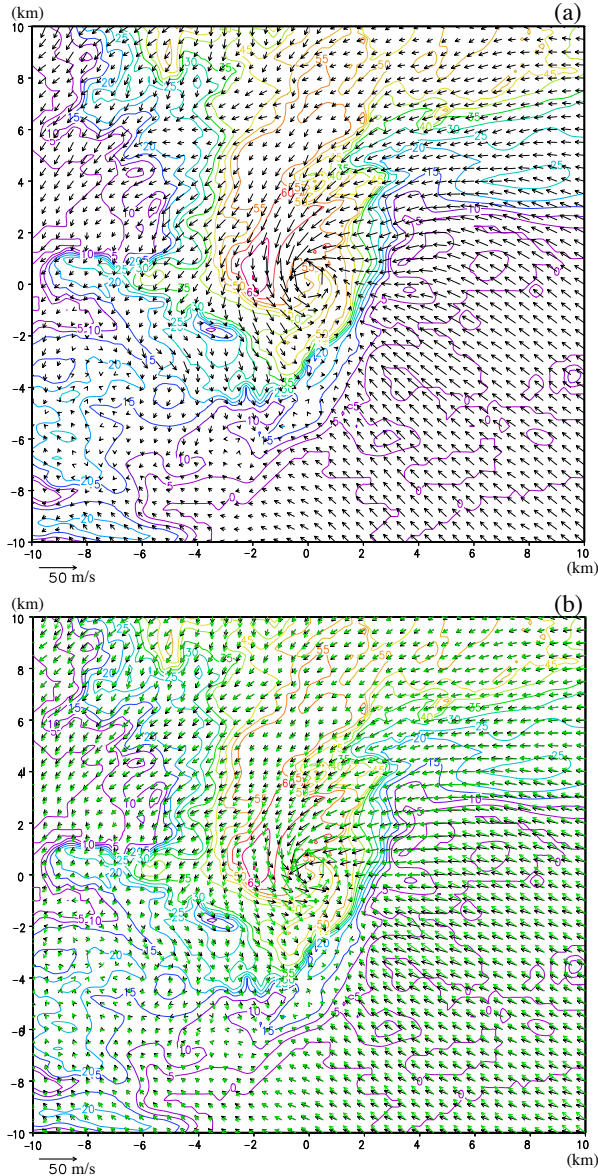


Fig. 2. (a) Model-simulated “true” vortex winds (black arrows) averaged over  $\tau = 60$  s. (b) Retrieved time-mean vortex winds (black arrows) versus the truth (green arrows) in (a). The vortex winds in (b) are retrieved by the extended method ( $\lambda = 1$ ) from simulated PAR radial-velocity and reflectivity scans (with the PAR located far east at 0.2 km height) every  $\Delta\tau = 10$  s over  $\tau = 60$  s. The color contours plot the reflectivity (in dBz).

### 5. Rapid adaptive scans for vortex wind analyses

The RMS errors of vortex winds retrieved by using 2 traces with different settings of  $\tau$  and  $\Delta\tau$  are listed in Table 2. As listed, the RMS error can be reduced if the scan rate is increased (from every 60 s to 30 s and 10 s) especially for  $\tau = 60$  s. The location error of the estimated vortex center is no larger than  $\Delta x/2 = 0.25$  km for the model-simulated vortex wind field. In real-data applications, the location errors often can be larger than 0.25 km (Xu et al. 2017b) and thus cause additional errors in retrieved vortex winds. Increasing the

scan rate adaptively (to every  $\Delta\tau = 10$  s) can reduce the location error of the estimated vortex center, especially when the movement (or trajectory) of the true vortex center is highly unsteady (or curved). The above results and their implications can be useful for designing PAR rapid scans adaptively for real-time vortex wind analyses.

Table 2. RMS errors (in  $\text{ms}^{-1}$ ) of vortex winds retrieved by using 2 traces with different settings of  $\tau$  and  $\Delta\tau$ .

	$\Delta\tau = 10$ s	$\Delta\tau = 30$ s	$\Delta\tau = 60$ s
$\tau = 30$ s	5.24	5.31	N/A
$\tau = 60$ s	4.59	4.68	5.09
$\tau = 120$ s	4.74	4.81	4.95

### Acknowledgments

We are thankful to Xiaobin Qiu for providing the SA code and to Nathan Snook and Tim Supinie for providing model-simulated fields in Fig. 2a. The research work was supported by the Warn-on-Forecast project at NSSL and the ONR Grant N000141410281 to University of Oklahoma (OU). Funding was also provided to CIMMS by NOAA/Office of Oceanic and Atmospheric Research under NOAA-OU Cooperative Agreement #NA17RJ1227, U.S. Department of Commerce.

### REFERENCES

- Purser, R. J., W.-S. Wu, D. F. Parrish, and N. M. Roberts, 2003: Numerical aspects of the application of recursive filters to variational statistical analysis. Part I: Spatially homogeneous and isotropic Gaussian covariances. *Mon. Wea. Rev.*, **131**, 1524–1535.
- Qiu and Xu 1992: A simple adjoint method of wind analysis for single-Doppler data. *J. Atmos. & Oceanic Technology*, **9**, 588–598.
- Qiu, X., Q. Xu, C. Qiu, K. Nai and P. Zhang, 2013: Retrieving 3-D wind field from phased-array radar rapid scans. *Advances in Meteorology*. vol. **2013**, Article ID 792631, 16 pages.
- Snook, N., Y. Jung, J. Brotzge, B. Putnam, and M. Xue, 2016: Prediction and ensemble forecast verification of hail in the supercell storms of 20 May 2013. *Wea. and Forecasting*, **31**, 811–825.
- Xu, Q., L. Wei and K. Nai, 2015: Analyzing vortex winds in radar observed tornadic mesocyclones for nowcast applications. *Wea. Forecasting*, **30**, 1140–1157.
- Xu, Q., L. Wei, and K. Nai, 2017a: Tornadic mesocyclone wind retrievals from radar observations. Extended abstract. *Special Symposium on Severe Local Storms: Observation needs to advance research, prediction and communication, 97th American Meteorological Society Annual Meeting*, 22–26 January 2017, Seattle, WA, Amer. Meteor. Soc., 928.
- Xu, Q., L. Wei and K. Nai, 2017b: A three-step method for estimating vortex center locations in four-dimensional space from radar observed tornadic mesocyclones. *J. Atmos. Oceanic Technol.*, **34**, 2275–2281.
- Xu, Q., L. Wei, K. Nai, S. Liu, R. M. Rabin, and Q. Zhao, 2015c: A radar wind analysis system for nowcast applications. *Advances in Meteorology*. vol. **2015**, Article ID 264515, 13 pages.